[1]Azlina Abdullah

[2*]Ismail Musirin

[3]Nor Azwan Mohamed Kamari

[4]Siti Rafidah Abdul Rahim

[5]Fathiah Zakaria

[6]Muhamad Hatta Hussain

[7]Nur Farahiah Ibrahim

Multi-Type Distributed Generation Installation under Load Variability for Loss Minimization in Distribution System

Abstract: - The increasing load demand in a power distribution network can lead to power loss increase, requiring the need for increased generation capacity. Therefore, it is necessary to take measures towards this situation, which can be referred to as a compensation process. An optimization process will be required to determine the optimal location and sizing of the compensation devices. The optimal sizing and location of the compensation devices will require an optimization process to ensure efficient, dependable and cost-effective operation. However, certain optimization techniques are prone to getting trapped in local optima and lack of exploration. This paper presents a new optimization technique to address multi-type distributed generation installation under load variability for loss minimization in distribution system. A strategy has been proposed to integrate the implementation of integrated strategy confining the standalone evolutionary programming (EP) and the proposed integrated immune moth flame evolutionary programming (IIMFEP) in one integrated algorithm. A common initialization process was adopted in both techniques, making it robust and intelligent in addressing the loss minimization issue in distribution system. Installations of DG Type-I and DG Type-III for loss minimization in distribution system under light load, full load and heavy load implemented in IEEE 69-Bus Radial Distribution System was considered in this study. The proposed IIMFEP managed to achieve 67.39% loss reduction for 3 units of DG Type-I installation and 97.62% loss reduction for 3 units of DG Type-III installation under light load condition. On the other hand, it achieves 69.14% loss reduction for 3 units of DG Type-I installation and 97.78% loss reduction for 3 units DG Type-III installation under full load condition. For the case of heavy load condition, the proposed IIMFEP managed to achieve 72.14% loss reduction for 3 units of DG Type-I installation and 98.03% loss reduction for 3 units DG Type-III installation. Obviously, the installation of 3 units of DG Type-III is superior to DG Type-I installation to achieve comparatively higher loss reduction. Comparative studies over the independent evolutionary programming (EP) and standalone moth flame optimization (MFO) technique revealed the merit of the proposed IIMFEP over EP and MFO.

Keywords: Distributed Generation, Evolutionary Programming, Loss Minimization, Moth Flame Optimization, Optimization techniques.

I. INTRODUCTION

The integration of distributed generation (DG) units into power distribution systems has become a pivotal strategy in modern power systems, aimed at improving reliability, reducing losses, and enhancing voltage stability. With the increasing penetration of renewable energy sources, optimizing the placement and sizing of DG units is crucial for maximizing these benefits while minimizing adverse effects, such as voltage fluctuations and power quality issues. A variety of optimization techniques have been developed to address these challenges, each with its strengths and limitations. Rahim et al. [1] explored the use of the Enhanced Memetic Evolutionary Firefly Algorithm with Artificial Neural Networks (EMEFA-ANN) for DG planning, focusing on minimizing distribution losses and increasing penetration levels. While effective, the complexity and computational demands of the method pose challenges for large-scale applications. In a similar study, Rahim et al. [2] assessed the performance of DGs in distribution networks, highlighting the potential of advanced optimization techniques. However, their approach required extensive computational resources and lacked adaptability to varying load conditions. Hamid et al. [3] employed a firefly algorithm combined with loss sensitivity analysis for optimal DG sizing, achieving improvements in voltage stability. Despite its efficiency, the algorithm's performance was sensitive to initial parameter settings, limiting its applicability in dynamic environments. Ahmad et al. [4] proposed Swarm Evolutionary Programming for loss minimization in photovoltaic-integrated systems. Although this approach demonstrated effectiveness, it faced challenges with scalability and handling diverse types of DGs. The resilience of power systems has also been a focus, with Zare-Bahramabadi et al. [5] and Ghasemi et al. [6] presenting

frameworks for enhancing distribution system resilience against natural disasters. These studies integrated risk-based dispatch and tie-line planning, but often overlooked the dynamic nature of load variability in their models. A comprehensive review by Ismail et al. [7] emphasized hybrid approaches for power loss reduction and voltage stability enhancement, advocating for the integration of multiple objectives to address modern power system complexities. Beza et al. [8] also highlighted the benefits of hybrid optimization methods for increasing DG penetration levels and reducing power losses.

Adajah et al. [9] provided a review on DG technologies, underscoring the importance of optimizing DG placement and sizing. However, their work primarily focused on technology review rather than optimization strategies. Various conference proceedings [10, 11, 14, 15, 20] have reported advancements in power system optimization, yet these sources often lack detailed methodological insights or comprehensive analyses of hybrid techniques. Kalpana et al. [12] introduced an Energy Efficient Squirrel Search Algorithm for cognitive wireless sensor networks, illustrating the potential of bio-inspired algorithms. Chuang et al. [16] improved the integrated transmission line transfer index for voltage stability, but their approach was limited to specific scenarios and did not address DG integration. Aljebreen et al. [13] examined the optimum allocation of distributed energy resources, focusing on voltage stability and loss reduction, though their study did not fully explore hybrid methods. Recent advancements in optimization techniques have been highlighted in works by Rautray et al. [17], Bharti et al. [18], and Hu et al. [19], who explored the application of squirrel search and hybrid algorithms for optimization problems. These studies demonstrate the effectiveness of bio-inspired algorithms but often lack comprehensive comparisons with established methods. Sakthivel et al. [21] tackled economic and emission dispatch problems using a multi-objective squirrel search algorithm, illustrating the potential of multi-objective optimization in power systems. Despite these contributions, the existing literature reveals several limitations. Many studies focus on specific optimization techniques, overlooking the potential benefits of combining multiple methods to address complex, multi-objective problems. Additionally, the adaptability and computational efficiency of these methods in dynamic environments with load variability remain significant challenges. The proposed Improved Memetic Firefly Evolutionary Programming (IMFEP) technique seeks to bridge this gap by enhancing convergence speed and solution quality compared to traditional Evolutionary Programming (EP) and Moth-Flame Optimization (MFO) algorithms. By leveraging the strengths of both EP and MFO, IMFEP offers a robust and efficient approach to multi-type multi-DG installation under load variability, ensuring minimized losses and improved voltage stability.

This paper presents an integrated optimization strategy to address multi-type distributed generation installation under load variability for loss minimization in distribution system. A strategy has been proposed confining the standalone evolutionary programming (EP) and the proposed integrated immune moth flame evolutionary programming (IIMFEP) in one integrated algorithm. A common initialization process was adopted in both techniques, making it robust and intelligent in addressing the loss minimization issue in distribution system. Installations of DG Type I and DG Type 3 for loss minimization in distribution system under light load, full load and heavy load implemented in IEEE 69-Bus Radial Distribution System (RDS).

II. DISTRIBUTED GENERATION

Distributed Generation (DG) is one of the compensation devices in power system. Other than DGs, we can also have flexible AC transmission devices (FACTs), capacitor banks placement, optimal reactive power dispatch (ORPD) or optimal transformer tap changer optimization (OTTCS). In this section, DG is described to give initial understanding to the readers. DGs can be installed either on the transmission or distribution systems. It is crucial to optimally locate the position of DG and to find the optimal sizing in power system since the non-optimality of integration of DG into the system may lead to possibility of under-compensation or over-compensation phenomena. DGs can be divided into 4 types i.e. Type 1, Type 2, Type 3 and Type 4 as reported in [5]. The detailed characteristics of DGs are tabulated in Table 1. For the DG Type 1, DG will have the capability to inject real power (P). The One important example for DG Type 1 is solar photovoltaic system where solar photovoltaic panels will convert sunlight into electrical energy. For DG Type 2, it has the capability to inject reactive power only (Q). On the other hand, DG Type 3 is capable to inject both the real power (P) and reactive power (Q) to a system. An example of DG type 3 is synchronous generator. Lastly, DG Type 4 has the capability of DG to inject real power

(*P*) but consumes reactive power (*Q*). In this study, DGs are installed in a distribution system, concerning DG Type 1 and DG Type 3.

Table 1: Different Types of Distributed Generations Characteristics

DG Type	Characteristics	Example	P_{DG}	Q_{DG}
Type-1	Delivering real power only.	Photovoltaic, fuel cells, micro-turbines.	1	0
Type-2	Deliver reactive power only.	Synchronous compensator, kVAr compensator, capacitors	0	1
Type-3	Deliver both real and reactive power.	Synchronous machines.	1	1
Type-4	Deliver real power but consume reactive power.	Induction generators used in wind farms.	1	-1

III. PROBLEM FORMULATION

The objective function of this study is to minimize the power system loss in the distribution systems. The total active power losses (APL), denoted as P_{LOSS} is the fitness function. In this study, the loss is computed by running a load flow study, in accordance to sweep feed forward load flow. The mathematical equation for power loss in the distribution system is represented by: -

$$P_{Loss} = \sum_{i}^{N} I_i^2 \ R_i \tag{1}$$

where *i* is the line number, I_i is the current that flows through line *i*, R_i is the resistance of line *i*, and *N* is the number of buses. The primary aim of this study is to minimize the overall active power loss in a distribution system. This objective is expressed mathematically as follows:

$$OF = \min \sum_{i=1}^{N} P_{loss\_i} \tag{2}$$

Two constraint equations, i.e. the equality and inequality constraint equations are addressed in terms of the voltage limit, the upper and lower limits of DG, and the total DG size. On the other hand, the equality constraint in this study is the power balance constraint.

Voltage constraints are given by:

$$0.95 \leq V_i \leq 1.05 \tag{3}$$

On the other hand, the upper and lower limits of DG can be written by: -

$$10\% \text{ of } P_{d\_total} \leq P_{DG\_i} \leq 80\% \text{ of } P_{d\_total} \tag{4}$$

$$10\% \text{ of } Q_{d\_total} \leq Q_{DG\_i} \leq 80\% \text{ of } Q_{d\_total} \tag{5}$$

The sum of real and reactive power output from the DG sources needs to be lower than the total power load demand of the system. The limits are in kW, kVar and kVA for Type I, II, III, and IV DG, respectively.

$$\sum_{i=2}^{N} P_{DG\_i} \leq P_{d\_total} \tag{6}$$

$$\sum_{i=2}^{N} Q_{DG\_i} \leq Q_{d\_total} \tag{7}$$

Power balance constraints [27]:

$$P_{substation} + \sum_{i=2}^{N} P_{DG} = P_{d\_total} + P_{loss} \quad (8)$$

$$Q_{substation} + \sum_{i=2}^{N} Q_{DG} = Q_{d\_total} + Q_{loss} \quad (9)$$

where V_i is voltage at bus *i*, P_{DG} is the DG active power, $P_{substation}$ and $Q_{substation}$ is the total real and reactive power injection by a substation into the network, P_{loss} and Q_{loss} are the total real and reactive power losses in the system, P_{DG_i} and Q_{DG_i} are the active and reactive power output of each DG unit at the *i-th* bus, meanwhile P_{d_total} and Q_{d_total} are the total active and reactive power load demand of the system.

IV. INTEGRATED COMBINED OPTIMIZATION STRATEGY

In this study, integrated optimization strategy is proposed as illustrated in the flowchart of Figure 1. The presentation integrates two parts, namely Part A and Part B. Part A shows the evolutionary programming (EP) algorithm, while Part B illustrates the integrated immune moth flame evolutionary programming (IIMFEP). The initialization process is the first step in both algorithms. Using random numbers, this process generates a population of candidates. In this procedure, the number of individuals, the size of each mutation step, the number of clones, and the maximum number of iterations had to be set. During the pre-fitness computation process, the fitness value of the random individuals is calculated. Individuals who violate the requirement are exterminated from the population. The accepted population is referred to as the parents' population. All the individuals will undergo a constraint violation test in order to filter all the unacceptable individuals. This will ensure that only the qualified individuals will undergo the next process. The unqualified individuals are rejected in this process. The random individuals represent nine control variables for DG Type-III and only 6 variables for DG Type-I. For DG Type-I, 3 control variables will be assigned for the random locations, while the other 3 control variables will be assigned for DG Type-I which is the real power. In DG Type-I, real power will be installed at a load bus as an additional supply to the original system. On the other hand, for DG Type-III, 3 control variables responsible to represent the random locations in the system, particularly at the load bus. The other 6 control variables will represent the real power and reactive power, emulating as additional supply to the system.

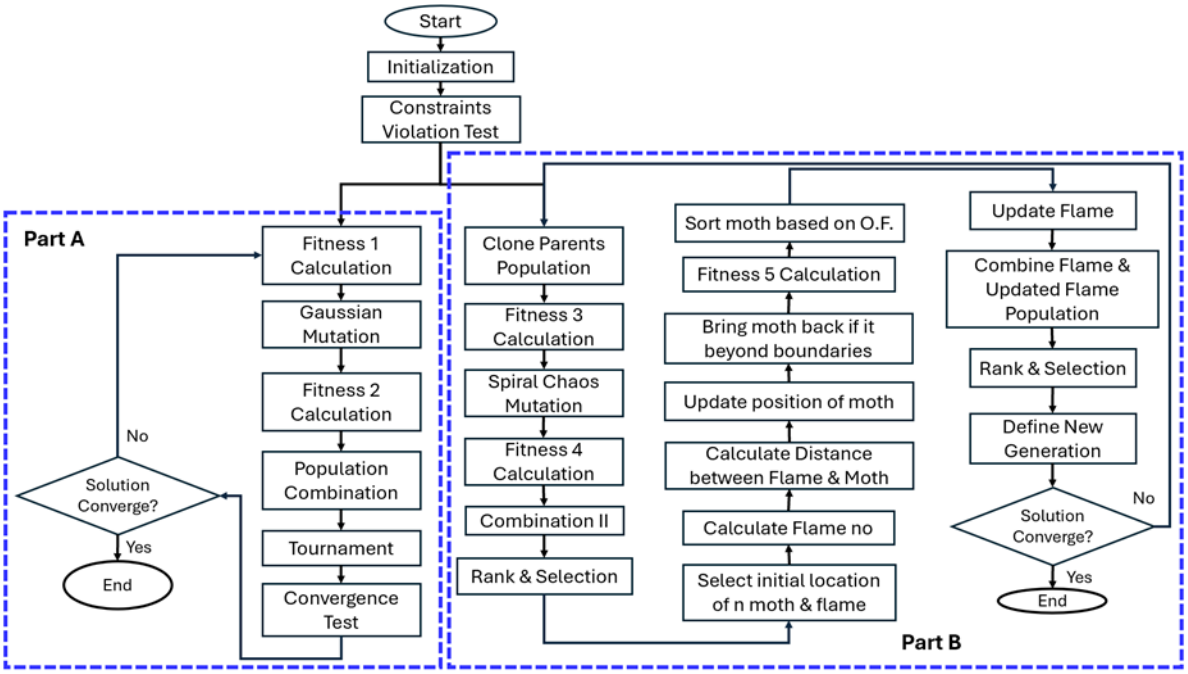

Figure 1: Proposed Integrated Optimization Strategy

The mathematical symbols for the real power, reactive power and locations are denoted as P_{g1}, P_{g2}, P_{g3}, Q_{g1}, Q_{g2}, Q_{g3}, Loc_1, Loc_2 and Loc_3. Each control will have several individuals. Conventionally, 20 individuals for each control variable are considered adequate to start with the optimization process. A higher number of individuals will lead to exhaustive optimization process and will not help the performance of the optimization solution. Apparently, the size of the matrix for the initialization process will be 20 by 9 for DG Type-III and 6 for DG Type-I. The remaining descriptions will be sub-divided for Part A and Part B separately.

Part A: Evolutionary Programming Part.

All the qualified and satisfied generated individuals will undergo Fitness I calculations, depending on the objective function specified in the problem formulation. Please take note that all the individuals have passed through the filtering process, where all these individuals will lead to power loss values less than the $loss_{set}$. $loss_{set}$ is calculated using the normal load flow, prior to the installation of DG into the system. Subsequent mutation process is performed to breed the offsprings or children, conducted using the Gaussian mutation operator. These offsprings subsequently went through Fitness II computation, which lead to similar matrix size as those in the Fitness I matrix. The next process is the population combination which causes the matrix size to be doubled, integrating the parents' population and the children population in cascode form. This connects both populations in parallel, i.e. top placement for the parent population and bottom placement for the children population. This combination does not vary the number of columns of the matrix or number of the control variables. In order to identify the survivors of the fittest, tournament or selection is performed to the combined population, making only half of the population to be prescribed as the next children for the next evolution. The stopping criterion designated for this process is defined by calculating the difference between the maximum and minimum fitness among all the combined individuals. For the first evolution (iteration), this difference is normally not yet met. After several evolutions or cycles of iterations, we will eventually see that this difference is less than the pre-determined value, known as the stopping criterion. The typical value is 0.00001 as defined by many previous works [1-10]. A converged solution will lead to similar values for all the control variables and the fitness values for each individual. Meaning to say that we will only see one value for each control variable, i.e. P_{g1}, P_{g2}, P_{g3}, Q_{g1}, Q_{g2}, Q_{g3}, Loc_1, Loc_2 and Loc_3. These are the optimal values for sizing and locations for the DGs to installed into the system.

Part B: Proposed IIMFEP Part

Part B explains the process of the proposed IIMFEP. The population of the parents is cloned by a chosen factor that multiplies these candidates. This multiplies the number of individuals. Cloned populations are used to produce offspring, bred during the mutation process. In the mutation process, Chaotic Local Search (CLS) mutation with circle map function is used to produce offspring. The offspring are produced by mutating the cloned population on the CLS operator specified in (16). X_{mut} is a new candidate solution or offspring.

$$X_{mut} = (1 - \lambda) * X_{clone} + \lambda * CH_i \quad (10)$$

where $i = 1, \ldots, K$, λ is a shrinking factor, which is defined as follows:

$$\lambda = (max_{cycle} - \ell + 1)/\, max_{cycle} \quad (11)$$

Here max_{cycle} is the maximum number of iterations and ℓ is the number of iterations. CH_k is the chaotic vector in the interval $[l, u]$, derived from:

$$CH_k = LB + chaos_k * (UB - LB) \quad (12)$$

Where $i = 1, \ldots, K$, UB and LB are the lower bound and upper bound of variable X, respectively. The individual produced by circle map function, $chaos_k$ is calculated as follows:

$$chaos_{k+1} = \{ chaos_k + b - (a\, 2\pi) \sin(2\pi\, chaos_k) \} \bmod (1) \quad (13)$$

Where $chaos_{k+1}$ is a new vector of individual in *k-th* generation produced by circle map function, $a = 0.5$ $b = 0.2$, k is the length of chaotic sequence and $ch0 \in (0, 1)$ is a random number. The fitness value of the offspring is then

computed during the Fitness 4 calculation. The cloned and offspring populations are merged into a single population via a combination process. A tournament system is used to determine the healthiest individuals in a population. First, the entire combined population is ranked, then the top two-thirds healthiest individuals are chosen and the remainder are removed. The moth population is then comprised of the top two-thirds of individuals. Once the moth and flame is initialize, the number of flames is computed as follows:

$$\text{flame } number = round\ (N_{flame} - \ell * \frac{N_{flame}-1}{T}) \quad (14)$$

The moth population is then updated using spiral equation:

$$S(M_i, F_j) = D_i \,.\, e^{bd}.\cos(2\pi t) \ + \ F_j \quad (15)$$

Then the algorithm constant b and d is updated. Constant b is the constant that defines the shape of logarithmic spiral and d is the random number in [r,1], where r is decreased linearly from -1 to -2. The distance between the moth and the flame is then computed as follows:

$$D_i = |\ F_j - M_i| \quad (16)$$

Where N_{flame} represents the maximum number of flames, T represents the maximum number of iterations, ℓ is the current number of iterations, F_j indicates the *j-th* flame and M_i indicate the *i-th* moth. Fitness 5 calculates the updated moth's fitness.

The optimization process employs a ranking mechanism, where new moths are sorted into corresponding new flames. The combination of both new and old flames forms a new population. After ranking this entire population, the 20 fittest individuals are selected through a tournament selection process, while the rest are discarded. These selected individuals serve as the parents for the next iteration. The convergence test evaluates whether the IIMFEP algorithm should be terminated upon reaching the maximum number of iterations. If the convergence conditions are not met, the process repeats. Fitness 3 is calculated to assess the fitness values of the cloned parents' population. The array size used to store these individuals is determined by multiplying the size of the parent population by the clone factor, which, when set to three, results in 60 individuals. A spiral chaos mutation is then applied to generate offspring, with the matrix size of the offspring being identical to that of the cloned parents. A subsequent fitness calculation is performed for the offspring population. The combination and selection stages, which involve Fitness 1 and Fitness 2 populations, are executed sequentially. The next step involves combining the populations of the parents and offspring, along with their respective fitness values. As in EP, this process increases the total number of individuals. For example, the original parent population has dimensions of 20 rows by 9 columns, while the offspring matrix has dimensions of 60 rows by 9 columns, resulting in a combined population of 80 rows by 9 columns.

The combined populations from Fitness 3, Fitness 4 and Fitness 5 undergo a tournament process to identify the fittest survivors. In this study, elitism is applied, where individuals are sorted based on their fitness values. Whether the sorting is in ascending or descending order depends on the objective function. For minimization objectives, individuals are ranked by the lowest fitness value, while for maximization, they are ranked by the highest fitness value. The convergence test serves as the stopping criterion for the optimization process. The maximum and minimum fitness values are evaluated from the combined matrix of Fitness 3, Fitness 4 and Fitness 5. The algorithm checks if these values are less than or equal to a threshold, typically 0.0001. If this condition is met, the optimization process is halted, indicating convergence has been achieved. However, if the condition is not satisfied, the process returns to the Fitness 1 calculation, allowing the surviving individuals to proceed to the next iteration of the optimization process.

V. RESULT AND DISCUSSION

Validation process was conducted on the IEEE 69-Bus Radial Distribution System. The radial distribution system has only a single source, while the rest of the buses are load buses. The single line diagram of the system is shown in Figure 2, while the detailed parameters are tabulated in Table 2. The results obtained from the study consider three cases as listed below: -

- Light load condition
- Full-load condition
- Heavy load condition

In a distribution system, the increment of load is impractically increased on only at the chosen buses or at a single bus. This will not affect much on the power flow in the system, unlike in the transmission system. Thus, the implementation of this study in radial distribution system is more effective when the three load conditions are considered stated before. The descriptions of the results will consider the three load conditions involving the installation of 3 units of DG Type-I and DG Type-III.

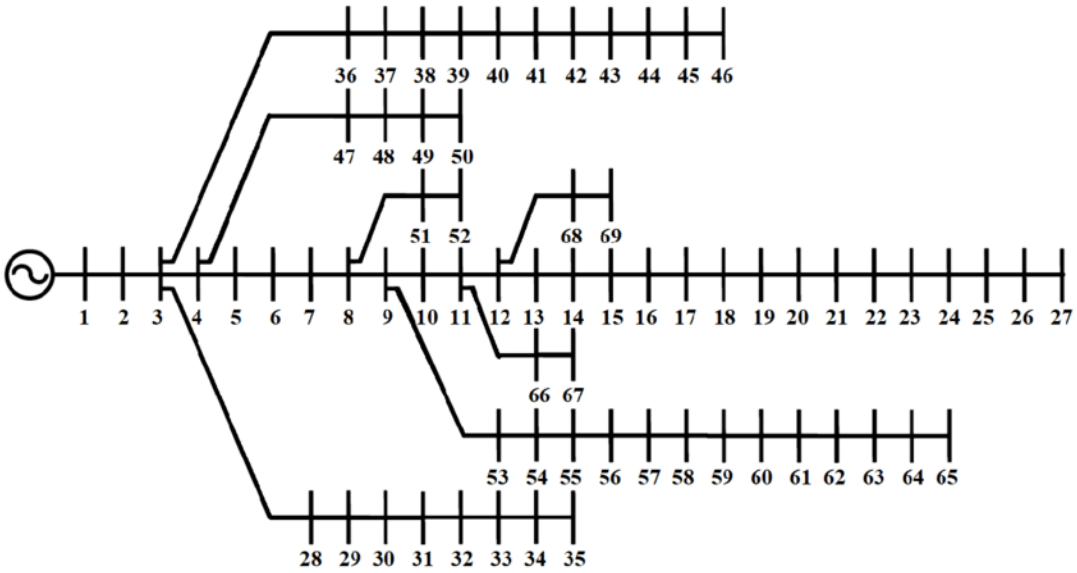

Figure 2: IEEE 69-Bus Radial Distribution System

A. Initialization Process.

The initialization process generates random individuals, each representing the locations, real power, and reactive power of the distributed generators (DGs) to be installed in the system. This section focuses on the initialization results for three DG units of both DG types under full-load conditions, with the goal of visualizing the randomness introduced during the process. Figure 3 presents a scatter plot illustrating the DG sizing and corresponding loss values during the initialization phase for 3 units of DG-Type-I under full-load conditions.

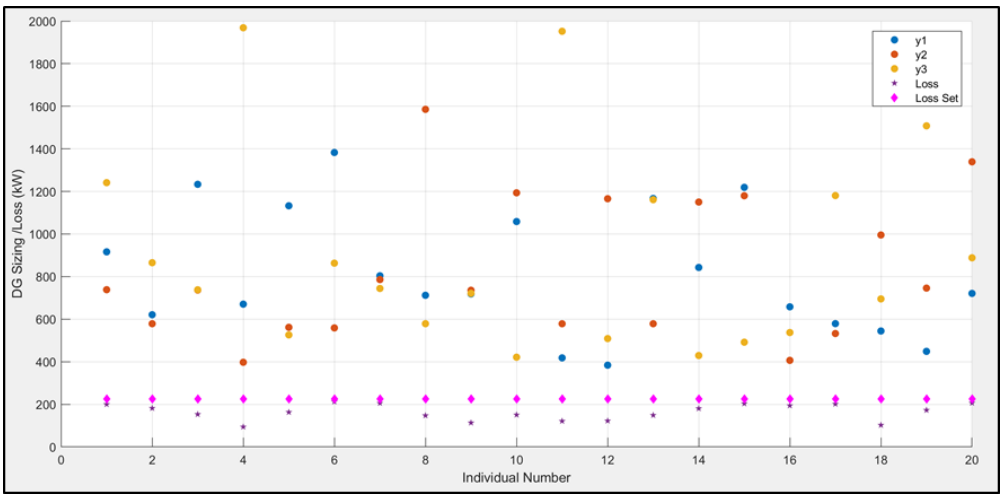

Figure 3: Scatter Plot for DG Sizing and Loss Values during initialization for 3-DG-Type 1 under Full-Load Condition

This figure illustrates the sizing of the real power injected into the system and the corresponding loss, represented as the fitness value, when DG Type-I is installed. It also displays the baseline *Loss_set* value, calculated from the normal load flow process before DG installation. The objective is for the post-installation loss values to be lower than *Loss_set*, a target successfully achieved during the initialization process. Each solution, or individual, in the scatter plot demonstrates a loss value lower than *Loss_set*, with three points representing the sizing of the three installed DG Type-I units. Although the initialization process involves randomness, all initial solutions manage to achieve low fitness values, indicating effective DG sizing and loss reduction.

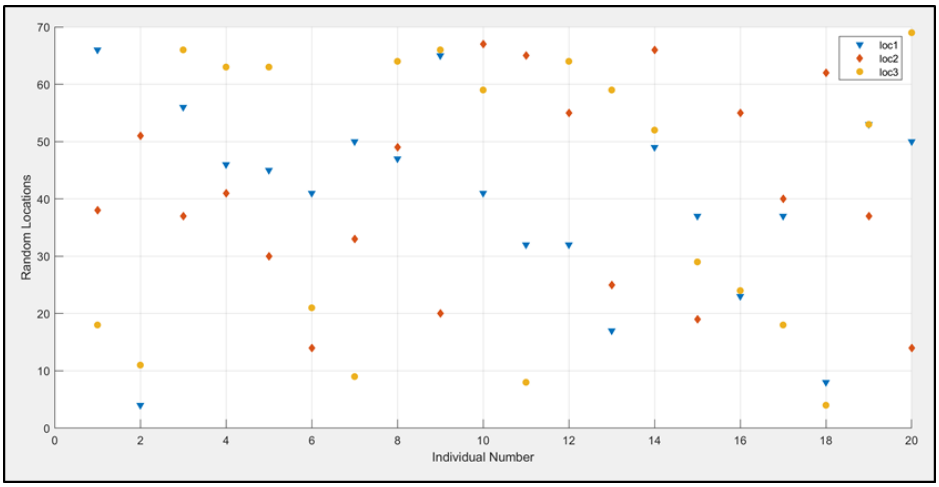

Figure 4: Scatter Plot for Random Locations during initialization for 3-DG-Type 1 under Full-Load Condition

Figure 5 presents a scatter plot depicting the DG sizing and loss values during the initialization process for three DG units of Type-III under full-load conditions. The figure illustrates the sizing of both real and reactive power to be injected into the system, alongside the corresponding loss values, which serve as the fitness values when the DG Type-III units are installed. Additionally, it displays the baseline *Loss_set* value, calculated before DG installation.

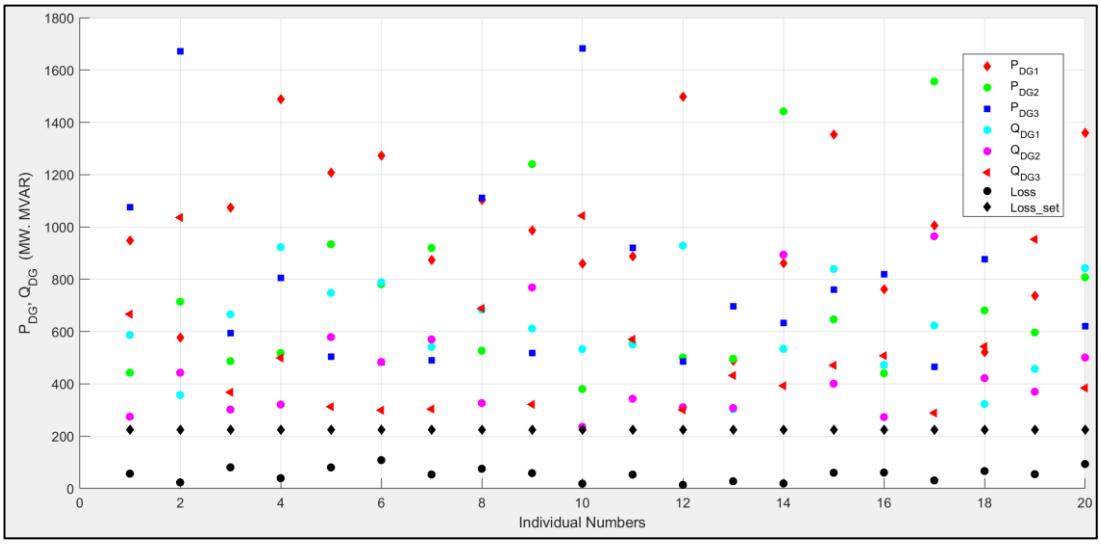

Figure 5: Scatter Plot for P_{DG1}, P_{DG2}, P_{DG3}, Q_{DG1}, Q_{DG2}, and Q_{DG3} during Initialization for 3-DG-Type III under Full-Load Condition

The *Loss_set* value represents the baseline system losses calculated through conventional load flow analysis. In this configuration, three control variables correspond to the real power (P_{DG}) of the distributed generators (DGs), and three control variables represent the reactive power (Q_{DG}) of the DGs to be installed. After the integration of Type-III DGs, the total system losses must be lower than the predefined *Loss_set* threshold. Each solution in the optimization successfully meets this requirement, exhibiting a loss value below *Loss_set*. The DG sizes for each

solution are plotted in a scatter plot, where each solution is represented by eight points—three for the sizing of P_{DG}, three for the sizing of Q_{DG}, and two for the associated loss values. Notably, every solution maintains losses consistently below the constant *Loss_set* value across all individuals.

Figure 6 illustrates a scatter plot of the random locations generated during the initialization phase for three units of DG Type-III under full-load conditions. These random locations are constrained between 2 and 69, corresponding to the 69 buses in the IEEE 69-Bus RDS, ensuring that all values are integers, reflecting the discrete nature of the bus system. Bus 1 is excluded from the DG placement because it serves as the main substation in the IEEE 69-Bus RDS, with its voltage typically fixed at 1.0 p.u.. At each initialization step, three distinct random locations—denoted as Loc_1, Loc_2, and Loc_3—are assigned. Loc_1 is allocated to DG unit P_{DG1} and its reactive power Q_{DG1}, Loc_2 to P_{DG2} and Q_{DG2}, and Loc_3 to P_{DG3} and Q_{DG3}. The installation of these three Type-III DG units ensures that total system losses are minimized and remain below the *Loss_set* threshold. It is essential to consider the relationship between Figures 5 and 6, as the random DG locations in Figure 6 are closely tied to the random sizing of DG units shown in Figure 5 during the initialization process.

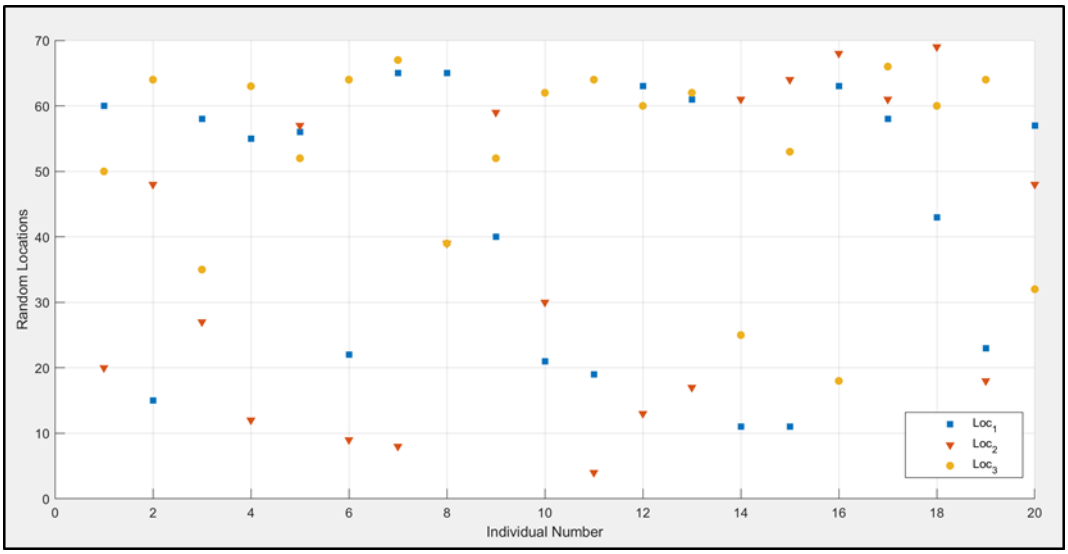

Figure 6: Scatter Plot for Random Locations during Initialization for 3-DG-Type III under Full-Load Condition

B: Light Load Condition

Under light load condition, the system operates below the full load specified by the manufacturer or utility. For this study, the total load is scaled using a load factor of 0.6 of the total load of the system during base case condition being validated on the IEEE 69-Bus RDS. Two independent DG installation schemes were evaluated, involving the installation of 3 units of DG Type-I and 3 units of DG Type-III, each implemented separately under this loading condition.

Table 3: Power Loss Minimization for 3 DG Type I Installation under Light Load

Parameter	Before	EP	MFO	IIMFEP
P_{LOSS} (kW)	75.53	27.08	24.72	24.63
Q_{LOSS} (kVAr)	34.45	13.5	12.46	12.43
CVD (p.u.)		0.3292	0.2799	0.272
V_{min} (p.u.)/Loc		0.9882/27	0.9873/65	0.9873/65
V_{max} (p.u.)/Loc		1.0000/1	1.0000/1	1.0000/1
Sizes of DGs (kW)/Loc	DG_1	234.30/13	1024.81/61	1019.84/61
	DG_2	1018.94/63	228.09/18	228.09/18
	DG_3	355.35/55	278.42/66	307.63/11
Total DG Sizes (kW)		1608.59	1531.32	1555.56

Table 3 presents the results of the compensation process for light load condition involving the installation of 3 DG Type-I units. With the application of the proposed IIMFEP technique, system power loss was reduced from 75.53 kW to 24.63 kW, representing a 67.39% reduction. By comparison, the EP and MFO methods reduced the power loss to 24.72 kW and 75.53 kW, respectively. The corresponding CVD achieved by IIMFEP is 0.272 p.u., as shown in the table. To achieve this, 1019.84 kW must be installed at Bus 61 (indicated by 1019.84/65), 228.09 kW at Bus 18 (228.09/18), and 307.63 kW at Bus 11 (307.63/11). Although IIMFEP outperformed both MFO and EP, its slight superiority highlights its value for improving distribution system efficiency, which has significant monetary implications for utilities. Detailed results for other parameters and techniques are also presented in the same table.

Table 4: Power Loss Minimization for 3 DG Type III Installation under Light Load

Parameter	Before	EP	MFO	IIMFEP
P_{LOSS} (kW)	75.53	5.11	1.8	1.8
Q_{LOSS} (kVAr)	34.45	3.97	2.54	2.54
CVD (p.u.)		0.154	0.03372	0.03390
V_{min} (p.u.)/Loc		0.9922/27	0.9966/50	0.9966/50
V_{max} (p.u.)/Loc		1.0032/63	1.0005/61	1.0005/61
Sizes of DGs (kW, KVAr)/Loc	DG_1	234.77/145.50/13	231.76/143.63/18	1046.84/648.77/61
	DG_2	1019.39/631.76/63	1046.79/648.75/61	309.11/191.57/11
	DG_3	355.60/220.38/55	309.40/191.75/11	231.85/143.69/18
Total DG Sizes (kW/kVAr)		1609.76/997.64	1587.96/984.13	1587.80/9840.30

Table 4 shows the results for the compensation process under light load conditions involving the installation of 3 DG Type-III units. With IIMFEP, the system power loss was dramatically reduced from 75.53 kW to 1.8 kW, representing a 97.61% reduction. This performance is comparable to MFO but significantly better than EP, which only reduced the loss to 5.11 kW. The corresponding CVD achieved is 0.03390 p.u., as shown in the table. To achieve this performance, 1019.84 kW and 648.77 kVAr must be installed at Bus 61 (indicated by 1046.84/648.77/61), while 309.11 kW and 191.57 kVAr must be installed at Bus 11 (309.11/191.57/11), and 231.85 kW and 143.69 kVAr at Bus 18 (231.85/143.69/18). Detailed results for other techniques are available in the same table. On the overall, it is worth to mention that the installation of 3 DG Type-III units demonstrates significantly superior performance compared to 3 DG Type-I units. Therefore, it is strongly recommended to prioritize the installation of DG Type-III units in the system, as the impact on performance is both substantial and demonstrably beneficial.

D: Full Load Condition

The second case investigates the full load condition with a load factor of 1.0, signifying that the total system load equals the base case load specified by the utility. Under this condition, the system's pre-distributed generation (DG) power load is 224.98 kW. Table 5 presents the outcomes for the installation of 3 units of DG Type-I. Utilizing the IIMFEP method, power losses were reduced to 69.42 kW. Similarly, the MFO technique achieved a comparable reduction, with a 69.14% decrease in power losses. In contrast, the EP approach reduced the power loss to 76.22 kW, corresponding to a 66.12% reduction. These results indicate that IIMFEP and MFO exhibit comparable performance, while IIMFEP demonstrates superiority over EP in reducing power losses. To accomplish these reductions, a total DG capacity of 2625.11 kW was required, distributed across three buses: 1718.64 kW at Bus 61, 380.88 kW at Bus 18, and 525.59 kW at Bus 11, as detailed in Table 5. These results align with those presented in Table 3 regarding optimal DG sizing and placement for the IIMFEP and MFO methods.

Additionally, the case study was extended to include the installation of 3 units of DG Type-III, with the results outlined in Table 6. Following the installation of DG Type-III units, IIMFEP and MFO reduced power losses to 5.00 kW from 224.98 kW, achieving a 97.81% reduction. EP, on the other hand, reduced power losses to 14.21 kW. To achieve this reduction, IIMFEP determined optimal placements of 1745.55 kW and 1081.79 kVAr at Bus 61,

515.89 kW and 319.72 kVAr at Bus 11, and 386.53 kW and 239.55 kVAr at Bus 18, as detailed in Table 6. The specific results for EP and MFO regarding DG sizing and location are also documented in the table.

Table 5: Power Loss Minimization for 3 DG Type I Installation under Full Load

Parameter	Before	EP	MFO	IIMFEP
P_{LOSS} (kW)	224.98	76.22	69.42	69.42
Q_{LOSS} (kVAr)	102.19	37.95	34.97	34.97
CVD (p.u.)		0.5611	0.4499	0.45
V_{min} p.u.)/Loc		0.9800/27	0.9790/65	0.9790/65
V_{max} p.u.)/Loc		1.0000/1	1.0000/1	1.0000/1
Sizes of DGs (kW)/Loc	DG_1	390.81/13	526.96/11	1718.64/61
	DG_2	1698.46/63	1718.87/61	380.88/18
	DG_3	592.28/55	380.15/18	525.59/11
Total DG Sizes (kW)		2681.55	2625.98	2625.11

Table 6: Power Loss Minimization for 3 DG Type III Installation under Full Load

Parameter	Before	EP	MFO	IIMFEP
P_{LOSS} (kW)	224.98	14.21	5	5
Q_{LOSS} (kVAr)	102.19	11.04	7.07	7.07
CVD (p.u.)		0.2577	0.05605	0.05610
V_{min} (p.u.)/Loc		0.9869/27	0.9943/50	0.9943/50
V_{max} (p.u.)/Loc		1.0052/63	1.0008/61	1.0008/61
Sizes of DGs (kW,KVAr)/Loc	DG_1	391.28/242.50/63	386.51/239.54/18	1745.55/1081.79/61
	DG_2	1699.00/1052.94/13	516.07/319.83/11	515.89/319.72/11
	DG_3	592.66/367.30/55	1745.55/1081.80/61	386.53/239.55/18
Total DG Sizes (kW/kVAr)		2682.94/1662.74	2648.14/1641.17	2647.97/1641.06

E: Heavy Load Condition

In the third case, the study examines the system under a heavy load condition, where the load factor is increased to 1.6. This elevated load factor results in significantly higher pre-optimization power losses compared to the light and full load scenarios. To assess the impact of different DG types, independent installations of similar DG units were performed. Table 7 presents the results for power loss minimization with the installation of 3 DG Type-I units under heavy load conditions. Before the DG installation, the system's power loss was recorded at 652.40 kW. Following optimization with IIMFEP, this loss was reduced to 181.77 kW, corresponding to a 72.14% reduction. In comparison, EP achieved a reduction to 199.36 kW, while MFO reduced the power loss to 182.36 kW. Although the performance of IIMFEP and MFO was similar, IIMFEP demonstrated a slightly better reduction in power loss. In contrast, IIMFEP outperformed EP with a greater margin. To achieve the 72.14% reduction, a total DG capacity of 4285.89 kW was installed across three buses: 2798.29 kW at Bus 61, 615.30 kW at Bus 18, and 872.30 kW at Bus 11.

The results for DG sizing and location are consistent with the presentations in Tables 3 and 5, while the optimization outcomes for EP and MFO are detailed in the same table. Furthermore, the study expanded to include the installation of 3 DG Type-III units under heavy load conditions, as shown in Table 8. The pre-optimization power loss remained the same at 652.40 kW. With the optimization of DG Type-III units using IIMFEP and MFO, the power loss was reduced to 12.85 kW, representing a 98.08% reduction. In contrast, EP only managed to reduce the power loss to

36.50 kW, nearly three times the loss minimized by IIMFEP and MFO. This clearly demonstrates that while IIMFEP and MFO performed comparably, they both significantly outperformed EP in minimizing power loss. The high degree of power loss reduction achieved by IIMFEP was accomplished through the installation of 2795.10 kW and 1732.25 kVAr at Bus 61, 826.70 kW and 512.34 kVAr at Bus 11, and 619.23 kW and 383.77 kVAr at Bus 18. Detailed optimization results for EP and MFO regarding DG sizing and location are available in the same table. A comparison of the results in Tables 7 and 8, which involve DG Type-I and DG Type-III installations, reveals that the inclusion of both real and reactive power elements in DG Type-III effectively enhances the overall power loss reduction. The installation of 3 DG Type-III units proves to be advantageous for the utility, potentially leading to significant cost savings.

Table 7: Power Loss Minimization for 3 DG Type I Installation under Heavy Load

Parameter	Before	EP	MFO	IIMFEP
P_{LOSS} (kW)	652.40	199.36	182.36	181.77
Q_{LOSS} (kVAr)	294.29	99.05	91.63	91.31
CVD (p.u.)		0.9288	0.7357	0.708
V_{min} (p.u.)/Loc		0.9672/27	0.9669/65	0.9669/65
V_{max} (p.u.)/Loc		1.0000/1	1.0000/1	1.0000/1
Sizes of DGs (kW,KVAr)/Loc	DG_1	626.35/13	2829.58/61	2798.29/61
	DG_2	2718.73/63	608.24/11	615.30/18
	DG_3	948.50/55	687.09/18	872.30/11
Total DG Sizes (kW/kVAr)		2681.55	4124.91	4285.89

Table 8: Power Loss Minimization for 3 DG Type III Installation under Heavy Load

Parameter	Before	EP	MFO	IIMFEP
P_{LOSS} (kW)	652.40	36.5	12.85	12.85
Q_{LOSS} (kVAr)	294.29	28.38	18.2	18.2
CVD (p.u.)		0.4148	0.08933	0.08920
V_{min} (p.u.)/Loc		0.9788/27	0.9908/50	0.9908/50
V_{max} (p.u.)/Loc		1.0081/63	1.0013/61	1.0013/61
Sizes of DGs (kW,KVAr)/Loc	DG_1	626.18/388.07/13	826.70/512.34/11	2795.10/1732.25/61
	DG_2	2718.54/1684.80/63	2795.04/1732.21/61	826.70/512.34/11
	DG_3	948.36/587.74/55	619.01/383.63/18	619.23/383.77/18
Total DG Sizes (kW/kVAr)		4293.09/2660.62	4240.75/2628.18	4241.03/2628.36

V. CONCLUSION

This paper has presented multi-type distributed generation installation under load variability for loss minimization in distribution system. Load variability is characterized by load factors ranging from 0.6 to 1.0 and 1.6, simulating light, full, and heavy load scenarios. The proposed IIMFEP optimization technique, which integrates moth-flame mutation into traditional evolutionary programming and incorporates a cloning process, has demonstrated significant effectiveness in minimizing power losses within the system. Two types of DG installations were studied: DG Type-I, which injects only real power into the system, and DG Type-III, which introduces both real and reactive power components. The study was validated using the IEEE 69-Bus Radial Distribution System, and the results show that DG Type-III outperformed DG Type-I in minimizing total power loss across light, full, and heavy load conditions. Comparative analyses of the IIMFEP, MFO, and EP optimization techniques indicate that while IIMFEP is comparable to MFO, it consistently outperforms EP, underscoring the effectiveness and uniqueness of IIMFEP in achieving superior results in power loss minimization.

ACKNOWLEDGMENTS

The authors would like to acknowledge the contribution and support by Universiti Teknologi MARA, Universiti Tenaga Nasional (UNITEN), Universiti Kebangsaan Malaysia (UKM) and Universiti Malaysia Perlis, Malaysia (UniMAP) for a joined research.

REFERENCES

[1] S. R. A. Rahim, I. Musirin, M. M. Othman, and M. H. Hussain, "Multiple DG planning considering distribution loss and penetration level using EMEFA-ANN method," Indones. J. Electr. Eng. Comput. Sci., vol. 7, no. 1, 2017, doi: 10.11591/ijeecs.v7.i1.pp1-8.

[2] S. R. A. Rahim, I. Musirin, M. H. Sulaiman, M. H. Hussain, and A. Azmi, "Assessing the performance of DG in distribution network," in 2012 IEEE International Power Engineering and Optimization Conference, PEOCO 2012 - Conference Proceedings, 2012. doi: 10.1109/PEOCO.2012.6230904.

[3] Z. B. A. Hamid, S. Jipinus, I. Musirin, M. M. Othman, and R. H. Salimin, "Optimal sizing of distributed generation using firefly algorithm and loss sensitivity for voltage stability improvement," Indones. J. Electr. Eng. Comput. Sci., vol. 17, no. 2, 2019, doi: 10.11591/ijeecs.v17.i2.pp720-727.

[4] N. Ameir Ahmad, I. Musirin, and S. I. Sulaiman, "Loss minimization of distribution system with photovoltaic injection using Swarm evolutionary programming," in Proceedings of the 2013 IEEE 7th International Power Engineering and Optimization Conference, PEOCO 2013, 2013. doi: 10.1109/PEOCO.2013.6564647.

[5] M. Zare-Bahramabadi, M. Ehsan, and H. Farzin, "A risk-based dispatchable distributed generation unit and tie line planning framework to improve the resilience of distribution systems," Sustain. Energy, Grids Networks, vol. 32, p. 100933, 2022, doi: 10.1016/j.segan.2022.100933.

[6] M. Ghasemi, A. Kazemi, E. Bompard, and F. Aminifar, "A two-stage resilience improvement planning for power distribution systems against hurricanes," Int. J. Electr. Power Energy Syst., vol. 132, no. December 2020, p. 107214, 2021, doi: 10.1016/j.ijepes.2021.107214.

[7] B. Ismail, N. I. Abdul Wahab, M. L. Othman, M. A. M. Radzi, K. Naidu Vijyakumar, and M. N. Mat Naain, "A Comprehensive Review on Optimal Location and Sizing of Reactive Power Compensation Using Hybrid-Based Approaches for Power Loss Reduction, Voltage Stability Improvement, Voltage Profile Enhancement and Loadability Enhancement," IEEE Access, vol. 8, no. December, pp. 222733–222765, 2020, doi: 10.1109/ACCESS.2020.3043297.

[8] Y.-C. H. and C.-C. K. Teketay Mulu Beza, "A Hybrid Optimization Approach for Power Loss Reduction and DG Penetration Level Increment in," Electr. Distrib. Network. Energies, vol. 22, no. 13, p. 6008, 2020.

[9] Y. Y. Adajah, S. Thomas, M. S. Haruna, and S. O. Anaza, "Distributed Generation (DG): A Review," in 2021 1st International Conference on Multidisciplinary Engineering and Applied Science, ICMEAS 2021, Institute of Electrical and Electronics Engineers Inc., 2021. doi: 10.1109/ICMEAS52683.2021.9692353.

[10] Siksha "O" Anusandhan University, Institute of Electrical and Electronics Engineers, Institute of Electrical and Electronics Engineers. Kolkata Section, and India. Department of Science and Technology, PCITC-2015 proceedings : 2015 IEEE Power, Communication and Information Technology Conference (PCITC) : 15-17 October, 2015, Siksha "O" Anusandhan University, Bhubaneswar, India.

[11] Chinese Association of Automation. Youth Academic Annual Conference (33rd : 2018 : Nanjing Shi, M. IEEE Systems, Chinese Association of Automation, and Institute of Electrical and Electronics Engineers, Proceedings, 2018 33rd Youth Academic Annual Conference of Chinese Association of Automation : May 18-20, 2018, Nanjing, China.

[12] S. Kalpana, A. Deepika, and R. Arthi, "An Energy Efficient Squirrel Search Algorithm for Cognitive Wireless Sensor Networks," in 2021 International Conference on System, Computation, Automation and Networking, ICSCAN 2021, Institute of Electrical and Electronics Engineers Inc., Jul. 2021. doi: 10.1109/ICSCAN53069.2021.9526368.

[13] K. S. Aljebreen, A. E. Hussein, and M. A. Abido, "Optimum Allocation of Distributed Energy Resources for Voltage Stability Enhancement and Loss Reduction," in EUROCON 2023 - 20th International Conference on Smart Technologies, Proceedings, Institute of Electrical and Electronics Engineers Inc., 2023, pp. 227–232. doi: 10.1109/EUROCON56442.2023.10199025.

[14] Sri Eshwar College of Engineering, Institute of Electrical and Electronics Engineers, Institute of Electrical and Electronics Engineers. Madras Section, and IEEE Computer Society, 3rd International Conference on Advanced Computing and Communication Systems : ICACCS 2016 : January 22-23, 2016, "Sri Eshwar College of Engineering" Campus.

[15] Keonjhjar. D. of E. E. Government College of Engineering, Keonjhjar. D. of C. S. and E. Government College of Engineering, Institute of Electrical and Electronics Engineers. Kolkata Section. Bhubaneswar Subsection, and Institute of Electrical and Electronics Engineers, International Conference on Computational Intelligence for Smart Power System and Sustainable Energy (CISPSSE-2020) : (29-31, July 2020).

[16] S. J. Chuang, C. M. Hong, and C. H. Chen, "Improvement of integrated transmission line transfer index for power system voltage stability," International Journal of Electrical Power and Energy Systems, vol. 78, pp. 830–836, Jun. 2016, doi: 10.1016/j.ijepes.2015.11.111.

[17] R. Rautray et al., "ASSIE: Application of Squirrel Search Algorithm for Information Extraction Problem," in 2021 International Conference in Advances in Power, Signal, and Information Technology, APSIT 2021, Institute of Electrical and Electronics Engineers Inc., 2021. doi: 10.1109/APSIT52773.2021.9641165.

[18] Bharti, B. Biswas, and K. K. Shukla, "QL-SSA: An Adaptive Q-Learning based Squirrel Search Algorithm for Feature Selection," in 2022 IEEE Congress on Evolutionary Computation, CEC 2022 - Conference Proceedings, Institute of Electrical and Electronics Engineers Inc., 2022. doi: 10.1109/CEC55065.2022.9870311.

[19] H. Hu, L. Zhang, Y. Bai, P. Wang, and X. Tan, "A Hybrid Algorithm Based on Squirrel Search Algorithm and Invasive Weed Optimization for Optimization," IEEE Access, vol. 7, pp. 105652–105668, 2019, doi: 10.1109/ACCESS.2019.2932198.

[20] Sichuan Institute of Electronics and Institute of Electrical and Electronics Engineers, 2018 IEEE 4th International Conference on Computer and Communications (ICCC) : December 7-10, 2018, Chengdu, China.

[21] V. P. Sakthivel, M. Suman, and P. D. Sathya, "Combined economic and emission power dispatch problems through multi-objective squirrel search algorithm," Appl Soft Comput, vol. 100, Mar. 2021, doi: 10.1016/j.asoc.2020.106950.

Table 2: System Data for IEEE 69-Bus Radial Distribution System (Bus 1 to Bus 34)

Branch Number	Sending Bus No.	Receiving Bus No.	Resistance (Ω)	Reactance (Ω)	Load at Receiving End Bus	
					Real Power (kW)	Reactive Power (kVAr)
1	1	2	0.0005	0.0012	0	0
2	2	3	0.0005	0.0012	0	0
3	3	4	0.0015	0.0036	0	0
4	4	5	0.0251	0.0294	0	0
5	5	6	0.366	0.1864	2.6	2.2
6	6	7	0.3811	0.1941	40.4	30
7	7	8	0.0922	0.047	75	54
8	8	9	0.0493	0.0251	30	22
9	9	10	0.819	0.2707	28	19
10	10	11	0.1872	0.0691	145	104
11	11	12	0.7114	0.2351	145	104
12	12	13	1.03	0.34	8	5.5
13	13	14	1.044	0.345	8	5.5
14	14	15	1.058	0.3496	0	0
15	15	16	0.1966	0.065	45.5	30
16	16	17	0.3744	0.1238	60	35
17	17	18	0.0047	0.0016	60	35
18	18	19	0.3276	0.1083	0	0
19	19	20	0.2106	0.069	1	0.6
20	20	21	0.3416	0.1129	114	81
21	21	22	0.014	0.0046	5.3	3.5
22	22	23	0.1591	0.0526	0	0

23	23	24	0.3463	0.1145	28	20
24	24	25	0.7488	0.2745	0	0
25	25	26	0.3089	0.1021	14	10
26	26	27	0.1732	0.0572	14	10
27	3	28	0.0044	0.0108	26	18.6
28	28	29	0.064	0.1565	26	18.6
29	29	30	0.3978	0.1315	0	0
30	30	31	0.0702	0.0232	0	0
31	31	32	0.351	0.116	0	0
32	32	33	0.839	0.2816	14	10
33	33	34	1.708	0.5646	19.5	14
34	34	35	1.474	0.4673	6	4

Table 2 (continue..):System Data for IEEE 69-Bus Radial Distribution System (Bus 35 to Bus 68)

Branch Number	Sending Bus No.	Receiving Bus No.	Resistance (Ω)	Reactance (Ω)	Load at Receiving End Bus	
					Real Power (kW)	Reactive Power (kVAr)
35	3	36	0.0044	0.0108	26	18.55
36	36	37	0.064	0.1565	26	18.55
37	37	38	0.1053	0.123	0	0
38	38	39	0.0304	0.0355	24	17
39	39	40	0.0018	0.0021	24	17
40	40	41	0.7283	0.8509	1.2	1
41	41	42	0.31	0.3623	0	0
42	42	43	0.041	0.0478	6	4.3
43	43	44	0.0092	0.0116	0	0
44	44	45	0.1089	0.1373	39.22	26.3
45	45	46	0.0009	0.0012	39.22	26.3
46	4	47	0.0034	0.0084	0	0
47	47	48	0.0851	0.2083	79	56.4
48	48	49	0.2898	0.7091	384.7	274.5
49	49	50	0.0822	0.2011	384	274.5
50	8	51	0.0928	0.0473	40.5	28.3
51	51	52	0.3319	0.1114	3.6	2.7
52	9	53	0.174	0.0886	4.35	3.5
53	53	54	0.203	0.1034	26.4	19
54	54	55	0.2842	0.1447	24	17.2
55	55	56	0.2813	0.1433	0	0
56	56	57	1.59	0.5337	0	0
57	57	58	0.7837	0.263	0	0
58	58	59	0.3042	0.1006	100	72
59	59	60	0.3861	0.1172	0	0
60	60	61	0.5075	0.2585	1244	888
61	61	62	0.0974	0.0496	32	23
62	62	63	0.145	0.0738	0	0
63	63	64	0.7105	0.3619	227	162

64	64	65	1.041	0.5302	59	42
65	11	66	0.2012	0.0611	18	13
66	66	67	0.0047	0.0014	18	13
67	12	68	0.7394	0.2444	28	20
68	68	69	0.0047	0.0016	28	20
			Total Load		3801.49	2694.6